Frequency Dependence in Double Layers in Polymer Light Emitting Diodes Based on Poly[(9,9-dioctylfluorenyl-2,7-diyl)-*co*-(1,4-phenylene)]/ [Poly-(9,9-dioctylfluorene-2,7-diyl-*co*-benzothiadiazole)]

A. Yusoff,*,† O. Brian,† and Z. Yusoff‡

OSRAM Opto Semiconductors GmbH, Wernerwekstrasse 2, D-93049 Regensburg, Germany, and 1. Physikalisches Institut, Universität Stuttgart, Pfaffenwaldring 57, 70550 Stuttgart, Germany

Received: August 31, 2006; In Final Form: October 25, 2006

For the EL two-layer devices two RC components are necessary for the description. In EL two-layer devices no indications of an insulating layer or a depletion region are found. During the measurements of the impedances of operated EL two-layer devices, under inert gas and in air, an increase of the resistance is observed. However, there are no signs for an insulating layer covering the entire contact area, through which the transport of charge carriers has to occur.

I. Introduction

During the past decade there has been lot of interest in the development of polymer light-emitting diodes (PLEDs) for display and backlighting purposes. PLEDs are self-emitting, have a very wide viewing angle, operate at lower voltages, and have bright emission. Due to these advantages, they have the potential to replace the current display technologies like the CRT (cathode ray tube) and LCDs (liquid crystal displays). Low-power bright colorful cell phones, television sets, laptop screens, automotive displays, and wearable electronic displays are some of the areas identified for the potential applications of these devices. However, some issues like electrical properties still need to be resolved before PLEDs reach their full potential market.

Recently reported[1−14] a combination of two polyfluorene-based polymers have been extensively studied in terms of the correlation between layer composition, morphology, and PLEDs properties. F8P poly[(9,9-dioctylfluorenyl-2,7-diyl)-*co*-(1,4-phenylene)][15] is known to be a high-mobility hole-transporting polymer, whereas F8BT [poly-(9,9-dioctylfluorene-2,7-diyl-*co*-benzothiadiazole)][16] shows a relatively high electron mobility. The ionization potentials were measured for 5.1 eV for F8P[15] and F8BT to be around 5.9 eV.[16−17] Assuming an exciton binding energy of 0.3 eV, the electron affinity can be calculated by subtracting this value and the optical band gap (2.4 eV for F8BT and 2.9 eV for F8P) from the ionization potentials. Following these arguments, F8BT should have the lowest unoccupied molecular orbital (LUMO) at 3.2 eV and the highest occupied molecular orbital (HOMO) at 5.9 eV, whereas F8P has a LUMO energy of 1.9 eV and a HOMO energy of 5.1 eV. Apparently, there exists a relatively large offset of 1.3 eV for the LUMO levels and of 0.8 eV for the HOMO levels, which guarantees very efficient electron dissociation at the interface.

Detail analysis revealed that the blend layers can be described by F8P-rich cylinders surrounded by a F8BT-rich matrix. Assuming the interface between these two phases to be cylindrical in shape with a height equal to the film thickness, a linear correlation was found between the interfacial area (per unit area of the layer) and the measured quantum efficiency. This is in accordance with the previously reported by Kietzke et al.[14] It was concluded that charges generated near this interface are efficiently transported through the corresponding F8P- or F8BT-rich phases. However, we note that the charges generated in the bulk are more susceptible for charge trapping due to the absence of a direct percolation path for charge transport. Higher efficiencies of up to 14% could only be reached by modifying the substrate by micro contact printing with self-assembled monolayers and using isodurene as the solvent.[2]

In conclusion, the results obtained by impedance spectroscopy are an important basis for the detailed description and interpretation of the electrical properties of the systems. From the information gained by impedance spectroscopy, equivalent circuits for an EL double-layer device can be devised. In addition, important conclusions on the distribution of the field strength within a sample can be drawn.

II. Experimental Detail

i. Sample Preparation of the Aqueous Polymer Dispersions. Preparation of F8P was published elsewhere[15] and F8BT dispersions were prepared via single-polymer solutions in chloroform (at 2.5 wt %), where F8BT were added to an aqueous sodium dodecyl sulfate (SDS) (100 mg of SDS/10 g of water) solution. After the mixture was stirred for 2 h for pre-emulsification, the miniemulsion was prepared by sonicating the mixture for 2 min. The samples were routinely left under stirring at 62 °C for 30 min to eliminate previous processing history. This was followed by ultrafiltration where the samples were left in centrifuge tubes (Amicon Ultra-4 centrifugal filter, 10000 molecular weight cutoff), to eliminate the excess of surfactant and concentrate the samples. The final dispersions had 7% of solid content and 5% SDS to the amount of polymer.

ii. Fabrication and Measurements of a Polymer Light Emitting Diodes Device. The devices under investigation consist of four layers on top of a glass substrate. As a bottom contact, the anode, a patterned ITO, is used which is optically transparent. The devices were fabricated on ITO substrates that had been ultrasonicated sequentially in detergent, deionized

* To whom correspondence should be addressed.
† OSRAM Opto Semiconductors GmbH.
‡ Universität Stuttgart.

10.1021/jp065665n CCC: $37.00
Published on Web 12/08/2006

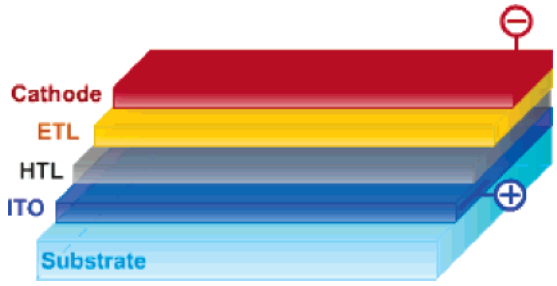

Figure 1. Schematic drawing of double-layer PLEDs.

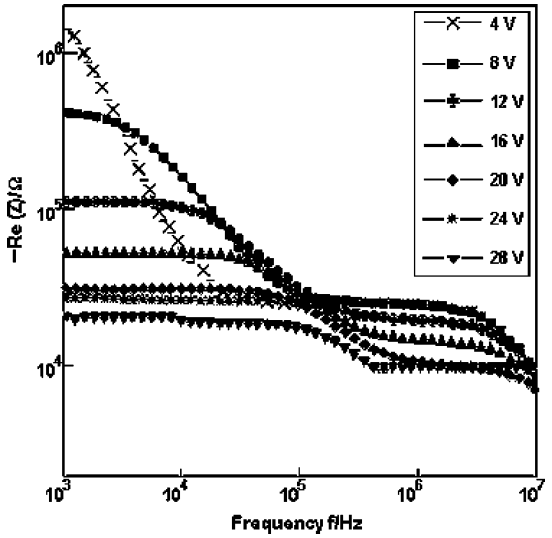

Figure 2. Real part of the impedance Re(Z) of an EL double-layer device as a function of the frequency f at different voltages.

water, 2-propanol, and acetone and had been treated with O_2 plasma for 10 min before use. All the evaporation of the metal electrodes was carried out in a vacuum evaporator inside an argon atmosphere drybox. A hole transport layer, poly[(9,9-dioctylfluorenyl-2,7-diyl)-*co*-(1,4-phenylene)] was spin-coated at a spin rate of 4000 rpm onto the ITO substrates and cured at 160 °C for 10 min under nitrogen. Then a layer of electron transport layer [poly-(9,9-dioctylfluorene-2,7-diyl-*co*-benzothiadiazole)] was spin-coated at 2000 rpm. The thickness of the films was measured on a Dektak 3030 surface profiler. A layer of 30-nm-thick magnesium (Mg) cathode was then vacuum-deposited at below 1×10^{-6} Torr through a mask. Typically, the deposition rate was between 0.1 and 0.5 nm/s. The device testing was carried out in air at room temperature. Such a PLED is shown in Figure 1. The impedance vs frequency curves were obtained by a high-frequency response analyzer (Schlumberger SI 1255).

III. Results and Discussion

Several characteristics for the impedance spectra of electroluminescent two-layer systems are shown. Figure 2 shows the real part Re(Z) of this EL two-layer device in a logarithmic logarithmic plot as a function of the frequency f at different voltages. In the region of low frequencies the spectra typically show frequency-independent behavior for voltages ≥8 V. Possibly this behavior also occurs for voltages <8 V at frequencies <1000 Hz. This frequency region, however, was not accessible with the employed instrument. With increasing voltages this plateau extends to larger frequencies (8 V, 10^3 Hz → 28 V, 10^5 Hz), with the value of Re(Z) decreasing for more than one magnitude (8 V, 4×10^5 Ω → 28 V, 2×10^4 Ω, for

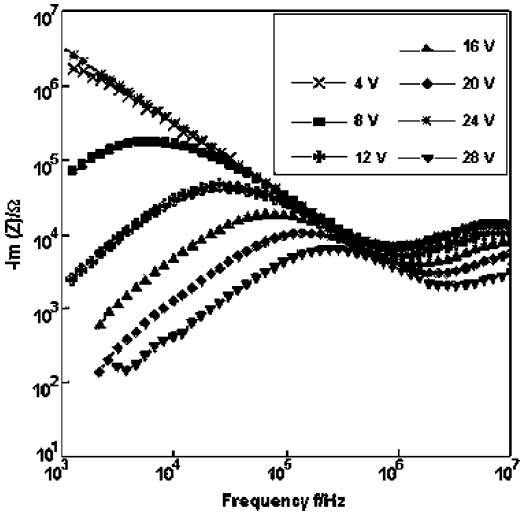

Figure 3. Imaginary part of the impedance Im(Z) of an EL double-layer device as a function of the frequency f at different voltages.

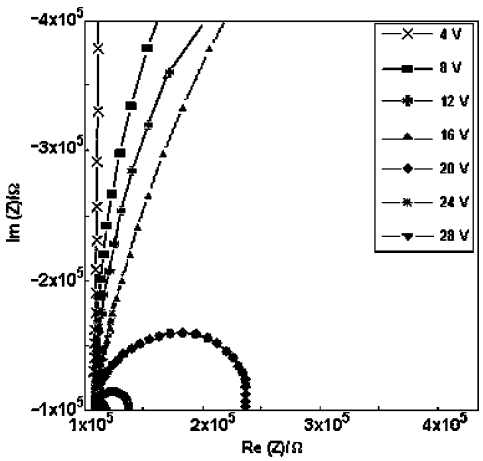

Figure 4. Real and imaginary parts of the impedance in the complex plane (Cole−Cole plot) of EL double-layer devices as a function of the frequency f at different voltages.

1000 Hz, respectively). A region adjoins, where the real part decreases with increasing frequency, before a second plateau is reached. The frequency of the transition into the second frequency-independent region shifts from $\sim 5 \times 10^4$ Hz at 4 V to $\sim 2 \times 10^6$ Hz at 28 V, and the value of the real part in this region is smaller for higher voltages. Between 2×10^6 and 5×10^6 Hz again a decrease of the Re(Z) values occurs.

The imaginary part Im(Z) (see Figure 3) also turns out to be strongly dependent on the voltage and shows an undulating behavior in this logarithmic logarithmic plot. Starting from small frequencies the imaginary part first increases and reaches a maximum, subsequently decreases, passes through a minimum, and then decreases again after a second increase at high frequencies. With increasing voltage both the maximum and the minimum (even though less clear in this logarithmic logarithmic plot) shift to higher frequencies, and the respective Im(Z) values decrease. Because of the limited measurement range the first maximum could only be detected starting from 8 V, and the second one only up to 12 V.

A clearer hint for a possible equivalent circuit in the form of a parallel connection of a capacitor and a resistor results from the plot of the real and imaginary parts in the complex plane (Cole−Cole plot, shown in Figure 4). Here the frequency f is contained as an implicit variable and increases from the right

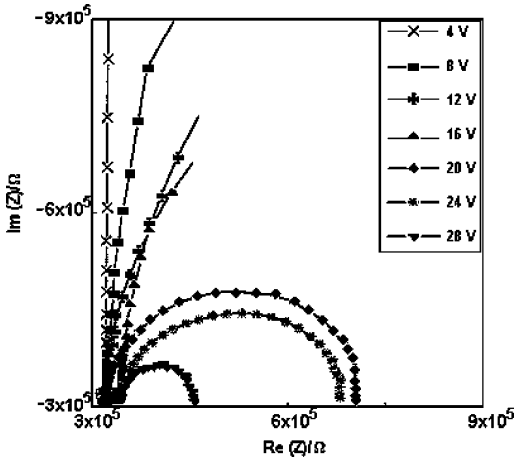

Figure 5. Voltage dependence of the real and imaginary part of the impedance (Cole−Cole plot) of an EL double-layer device before and after operation (28 h, j_{const}) 10 mA/cm^2). The same symbol shapes correspond to the same voltages, the open symbols denote the nonoperated contact, and the solid symbols denote the operated contact.

(1000 Hz) to the left (10 MHz). In contrast to the single-layer device, for the two-layer devices two semicircles appear.

For both the Re(Z)/f and the Im(Z)/f spectra of this EL two-layer devices two structures resembling relaxation are found for voltages ≥20 V. In addition, the Im(Z)/Re(Z) plots show two semicircles. These results show that for the description of this device at least two RC components are necessary. A more detailed discussion of the equivalent circuit and the resulting distribution of the field strength follow for further examples incorporating F8P in the hole-conducting blend system.

To our knowledge, impedance spectroscopical investigations for EL two-layer devices have yet been found in the literature. In this case, we assumed that the small semicircle at high frequencies is interpreted as bulk resistance, whereas the large semicircle at low frequencies is caused by the depletion region of the Schottky contact. Especially the large semicircle turns out to be strongly dependent on the voltage. At higher voltages, however, and as soon as electroluminescence occurs, it cannot be resolved anymore, due to the disappearance of the depletion region. Within a certain voltage range the F8P systems thus can also be regarded as "two-layer devices" (bulk and depletion region). This interpretation, however, cannot be applied for the PLEDs investigated in this work because neither any signs of the existence of a Schottky contact (insufficient diode behavior with rectification ratios of 10^3−10^4, too small dependence of the capacitance on the voltage) are present nor the blending together of the two semicircles in the impedance spectra is observed.

The explanations discussed in this section were confirmed by further measurements for EL two-layer devices with different hole-transporting blend devices. The results show that the assumptions with respect to the distribution of the field strength and the equivalent circuit can be applied to further EL two-layer devices incorporating this design.

The investigation of the impedance of samples after operation can clarify how the complex resistance is altered by the current flow and whether any changes in the equivalent circuit, such as additional RC components, result.

A standard EL two-layer device was operated for 28 h at a constant current density of 10 mA/cm^2 in a nitrogen atmosphere. In the course of operation the voltage increased from 8.6 to 10.9 V. Figure 5 shows the dependence of the Im(Z)/Re(Z) experimental curves of the contact before (open symbols) and after operation (solid symbols) on the voltage (the same symbol shapes correspond to the same voltages). Also after operation two semicircles still appear; however, the minimum is shifted to smaller Re(Z) values. Therefore, the second, smaller semicircle in the used contact can only be resolved rudimentarily. However, analogous to the nonoperated systems, two RC components suffice for the description of the equivalent circuit. In the large semicircles the increase of the complex resistance can be clearly seen since both the diameters and the positions of the zenith reach larger values. A comparison of the experimental curves of the operated contact starting from 20 V with the Im(Z)/Re(Z) curves of the non-operated contact, which are increased by 4 V, reflects very well the increase of the voltage which was measured during operation.

IV. Conclusions

In summary, we have elucidated the systematic analysis of electrical properties of polymer light emitting diodes at various frequencies. The results of the impedance spectroscopical investigations for EL two-layer devices can be summarized as follows: EL two-layer devices, two RC components, and one resistance caused by the experimental setup are necessary for the description of the equivalent circuit. The electric field decreases mainly over the vapor-deposited F8P layer.

The measurements of the impedances of operated EL two-layer devices both under inert gas and in air gave no indication of an insulating layer covering the entire contact area, through which the transport of charge carriers has to occur. The observed increase of the resistance can be explained by the thermally induced rearrangement of the molecules, such as dimerization or crystallization. These sites can act as traps for the charge carriers and lead to space charge effects, which again hinder the injection of charge carriers.[18] One further mechanism which may cause the increase of the voltage is the reduction of the effective contact area through which the transport of the charge carriers can proceed, e.g., by the partial oxidation of the cathode. Various electrical analyses of the devices will be explored in a future work.

Acknowledgment. Financial support from the IRPA Strategic Research and the Universität Stuttgart is gratefully acknowledged and thanks to Azlynn Alias for her technical assistance.

References and Notes

(1) Halls, J. J. M.; Arias, A. C.; MacKenzie, J. D.; Wu, W. S.; Inbasekaran, M.; Woo, E. P.; Friend, R. H. *Adv. Mater.* **2000**, *12*, 498−502.

(2) Arias, A. C.; Corcoran, N.; Banach, M.; Friend, R. H.; MacKenzie, J. D. *Appl. Phys. Lett.* **2002**, *80*, 1695−1697.

(3) Arias, A. C.; MacKenzie, J. D.; Stevenson, R.; Halls, J. J. M.; Inbasekaran, M.; Woo, E. P.; Richards, D.; Friend, R. H. *Macromolecules* **2001**, *34*, 6005−6013.

(4) Barker, J. A.; Ramsdale, C. M.; Greenham, N. C. *Phys. Rev. B* **2003**, *67*, 075205/1−9.

(5) Morteani, A. C.; Dhoot, A. S.; Kim, J.-S.; Silva, C.; Greenham, N. C.; Murphy, C.; Moons, E.; Cina, S.; Burroughes, H.; Friend, R. H. *Adv. Mater.* **2003**, *15*, 1708−1712.

(6) Ramsdale, C. M.; Bache, I. C.; MacKenzie, J. D.; Thomas, D. A.; Arias, A. C.; Donald, A. M.; Friend, R. H.; Greenham, N. C. *Physica E* **2002**, *14*, 268−271.

(7) Ramsdale, C. M.; Barker, J. A.; Arias, A. C.; MacKenzie, J. D.; Friend, R. H.; Greenham, N. C. *J. Appl. Phys.* **2002**, *92*, 4266−4270.

(8) Snaith, H. J.; Arias, A. C.; Morteani, A. C.; Silva, C.; Friend, R. H. *Nano Lett.* **2002**, *2*, 1353−1357.

(9) Stevenson, R.; Arias, A. C.; Ramsdale, C. M.; MacKenzie, J. D.; Richards, D. *Appl. Phys. Lett.* **2001**, *79*, 2178−2181.

(10) Stevens, M. A.; Silva, C.; Russel, D. M.; Friend, R. H. *Phys. Rev. B* **2001**, *63*, 165213−11652.1.

(11) Kietzke, T.; Neher, D.; Landfester, K.; Montenegro, M.; Güntner, R.; Scherf, U. *Nat. Mater.* **2003**, *2*, 408−412.

(12) Piok, T.; Gamerith, S.; Gadermaier, C.; Wenzl, F. P.; Patil, S.; Montenegro, R.; Kietzke, T.; Scherf, U.; Landfester, K.; Neher, D.; List, E. J. W. *Adv. Mater.* **2003**, *15*, 800−804.

(13) Landfester, K.; Montenegro, R.; Scherf, U.; Güntner, R.; Asawapirom, U.; Patil, S.; Neher, D.; Kietzke, T. *Adv. Mater.* **2002**, *14*, 651−655.

(14) Kietzke, T.; Neher, D.; Kumke, M.; Montenegro, R.; Landfester, K.; Scherf, U. *Macromolecules* **2004**, *37*, 4882−4890.

(15) Yusoff, A.; Hassan, Z.; Abu Hassan, H. *Appl. Phys. Lett.* **2006**, *88*, 242109.

(16) Campbell, A. J.; Bradley, D. D. C.; Antoniadis, H. *Appl. Phys. Lett.* **2001**, *79*, 2133−2135.

(17) Fung, M. K.; Tong, S. W.; Lai, S. L.; Bao, S. N.; Lee, C. S.; Wu, W. W.; Inbasekaran, M.; O'Brien, J. J.; Liu, S. Y.; Lee, S. T. *J. Appl. Phys.* **2003**, *94*, 2686−2694.

(18) Wakimoto, T.; Kawami, S.; Nagayama, K.; Yonemoto, Y.; Murayama, R.; Funaki, J.; Sato, H.; Nakada, H.; Imai, K. International Symposium of Inorganic and Organic Electroluminescence, Hamamatsu, Japan, 1994.